

Slip at the liquid-liquid interface

Joel Koplik*

*Benjamin Levich Institute and Department of Physics,
City College of the City University of New York, New York, NY 10031*

Jayanth R. Banavar†

Department of Physics, The Pennsylvania State University, University Park, PA 16802

(Dated: November 28, 2019)

The conventional boundary conditions at the interface between two flowing liquids include the continuity of the velocity field. As in the liquid-solid case, continuity of the tangential component of velocity is not obvious, and we have undertaken molecular dynamics simulations of the Couette and Poiseuille flows of two-layered liquid systems with various molecular structures and interactions. In all cases, the average velocity is found to vary continuously across the interface. However, when the total liquid density in the interfacial region drops significantly compared to the bulk values, the tangential velocity varies very rapidly there, and would appear discontinuous at a coarse or continuum resolution. The value of this apparent slip varies linearly with the shear stress at the interface, with a constant of proportionality depending on the nature of both liquids but not the flow configuration. Thus, a version of the Navier boundary condition appears to apply in this situation.

PACS numbers: 47.10.+g,47.11.+j,47.45.Gx,68.05.-n

Recent studies of the nanoscale behavior of flowing fluids have reinvigorated interest in the nature and validity of the boundary conditions which accompany the Navier-Stokes equations. The velocity condition at a solid-liquid interface, and the possibility of slip there, has been a particular focus [1] due to its relevance in possible “lab on a chip” and other devices[2, 3]. Although the no-slip condition on the tangential velocity has been widely accepted for over a century, recent experiments and molecular dynamics simulations have observed liquid-solid slip in several situations, notably strongly hydrophobic surfaces, gas bubbles or perhaps gas layers at the solid surface, pillared surface geometries, and polymeric liquids. Intuitively, a no-slip condition would naturally arise when the liquid molecules crowd against the solid surface and interact strongly with the spatially corrugated potential produced by atoms in the solid. The first four situations where slip arises all lack this feature, as does a *gas*-solid interface where slip is well known to occur [4]. In the polymer case there are competing explanations for wall slip [5], but all involve poor adhesion of the bulk liquid to the wall region.

At a liquid-liquid interface the conventional boundary condition is also no-slip. An obvious physical argument is that the interface between the two liquids is actually a region whose thickness is at least a few molecular diameters, where molecules of both materials are present and interacting with each other. It is difficult to imagine how two intermixed dense liquids could maintain distinct molecular speeds, and one expects a single velocity for both liquids in the interface, and that this velocity would vary smoothly in moving from the interface into either bulk region as the species concentrations change gradually. In the light of the examples of solid-liquid slip cited above, this argument might fail when interfacial mixing

is poor and the molecules of different species are spatially separated. For simple liquids, we are not aware of any experimental measurements or systematic computational studies of liquid-liquid slip at all, although for polymer melts there is by now convincing indirect [6] and direct [7] evidence for slip. The former study is based on the interpretation of measurements of pressure drop *vs.* shear rate in extrusion, and the latter on confocal microscopic observation with a spatial resolution of about 10μm, but there is no molecular-scale information available.

To investigate the question of liquid-liquid slip on a fundamental microscopic basis, we have conducted molecular dynamics (MD) simulations of the Couette and Poiseuille flows of two-layered immiscible liquid systems for a number of simple choices of interactions and molecular architecture. Standard MD techniques [8, 9] are used, and the computational details are similar to those of Refs. [10]. The basic interatomic potential of Lennard-Jones form, $V_{ij}(r) = 4\epsilon \left[(r/\sigma)^{-12} - A_{ij}(r/\sigma)^{-6} \right]$, where r is the interatomic separation, σ is roughly the size of the repulsive core, of order a few Angstroms, ϵ is the strength of the potential and $A_{ij} = A_{ji}$ is a dimensionless parameter that controls the attraction between atoms of atomic species i and j . Numerical results are expressed in terms of the length scale σ (a few Angstroms), the atomic mass m , and a time scale $\tau = \sigma(m/\epsilon)^{1/2}$, a few picoseconds. Temperature is controlled by a Nosé-Hoover thermostat, and the atoms are in many cases grouped into flexible chain molecules using a FENE potential $V_{\text{FENE}}(r) = -(k/2) \ln \left[1 - r^2/r_0^2 \right]$ with maximum bond length $r_0 = 1.5\sigma$ and spring constant $k = 30\epsilon/\sigma^2$. The liquids are confined between solid walls, each made of a layer of fcc unit cells whose atoms are tethered to lattice sites with a stiff linear spring. Periodic boundary conditions are applied in the two lateral directions. Cou-

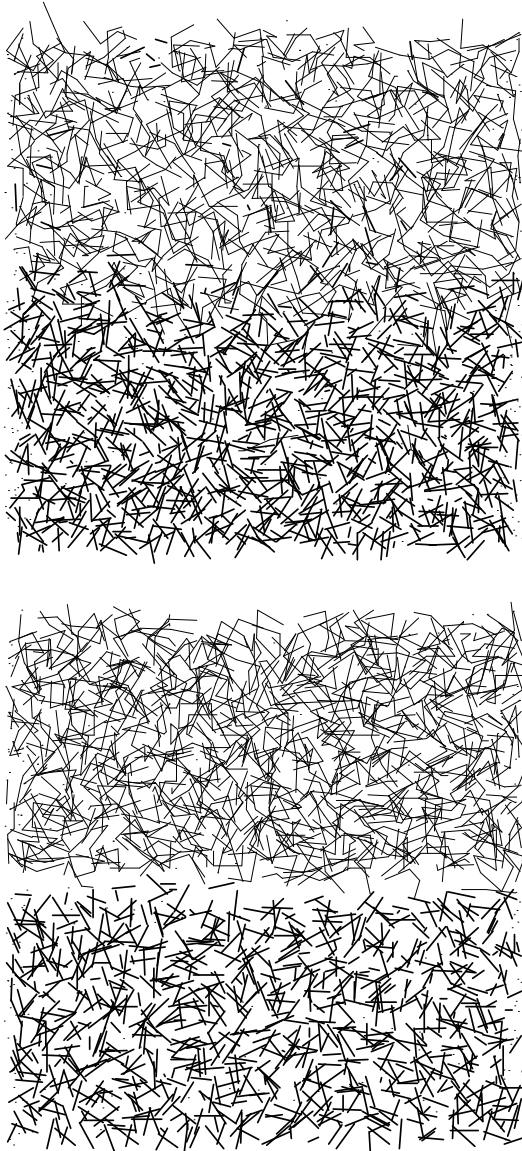


FIG. 1: Interfacial region for the (2,4) system for miscible (top) and immiscible (bottom) interactions. The figure shows a three dimensional slab centered on the interface, as viewed from a long distance. Molecules are represented by the line segments joining the atomic centers, using thick/thin lines for dimer/tetramer molecules. The width of the system is 17.1σ , and the instantaneous gap between the upper and lower liquids in the immiscible case is $0.5\text{--}1.0\sigma$.

ette flow is achieved by translating the upper and lower wall tether sites at constant velocity $\pm U$, and Poiseuille flow results from applying an acceleration g parallel to the walls to each liquid atom.

The different simulated systems are characterized by the interaction coefficients A_{ij} and the lengths ℓ_1 and ℓ_2 – the number of atoms per chain – of the two species of liquid molecule. The interactions are either immiscible, with $A_{12} = 0$ and all other $A_{ij} = 1$, or partially miscible as given by the Lorentz-Berthelot combination rules [8],

with $A_{11} = 5/4$, $A_{22} = 3/4$, and $A_{12} = \sqrt{A_{11}A_{22}} = 0.97$. Although the interactions are somewhat simplified as compared with realistic molecules, these systems exhibit a sufficient variety of behaviors to identify some trends. We have examined systems with both types of interactions, for the cases $(\ell_1, \ell_2) = (1, 1)$, $(2, 4)$ and $(4, 16)$. In the first two cases, the simulated system consists of 4000 atoms of each fluid, and 576 solid atoms in each wall, and has length 17.1σ in the flow and neutral directions and 34.2σ between walls; the third system was twice as large in each dimension and has eight times the number of atoms. The simulated Reynolds numbers are $O(10^{-2} - 1)$, and the Deborah number based on the characteristic atomic time τ is $\text{De} = \dot{\gamma}\tau = O(10^{-2})$. We will discuss the results for the prototypical $(2,4)$ case in some detail, with comparative comments on the others. Numerical results are summarized in Table I below.

A crucial feature of these two-liquid systems is the microscopic structure of the interface, and in Fig. 1 we show a snapshot of the atoms in this region for the miscible and immiscible cases. In the miscible case atoms of the two molecules attract each other, so an overlap region separates the bulk liquids, whereas in the immiscible case the two types of atom repel each other, and there is an open gap. The time-averaged density profiles in Fig. 2 reflect this behavior: in the miscible case the density varies monotonically from one bulk value to the other whereas the immiscible case shows a substantial dip in density in the interfacial region. A quantitative measure of this density dip used below is the the difference between the mean of the two bulk densities and the density at the interface, relative to the mean, $\delta = 0.66$ in this case. In Couette flow, we see that the velocity profile for the miscible system consists of two straight segments with different slopes (reflecting the different viscosities of the two liquids) with a rounded transition located at the position of the interface. The shear stress (not shown) has a constant value throughout both liquids. In Poiseuille flow for the miscible system, the density profile is essentially unchanged, while the velocity profile Fig. 3 corresponds to two distinct parabolas with a smooth transition, and the shear stress has two straight segments of different slope (reflecting the different liquid densities) which join smoothly to produce a continuous function of position.

In the immiscible case, while the velocity profiles are again continuous functions, they exhibit a very rapid transition in traversing the interface in both flows, while the shear stress has the same qualitative features as in the previous case. Note that in obtaining these density, velocity and stress profiles, we divide the region between the walls into *very* narrow slabs of thickness 0.17σ parallel to the interface and average over a 5000τ time interval. Most conceivable experiments and all continuum modeling will not have the sub-Angstrom spatial resolution of these simulations, and the smoothed step in the velocity field in the immiscible case would appear to be a discon-

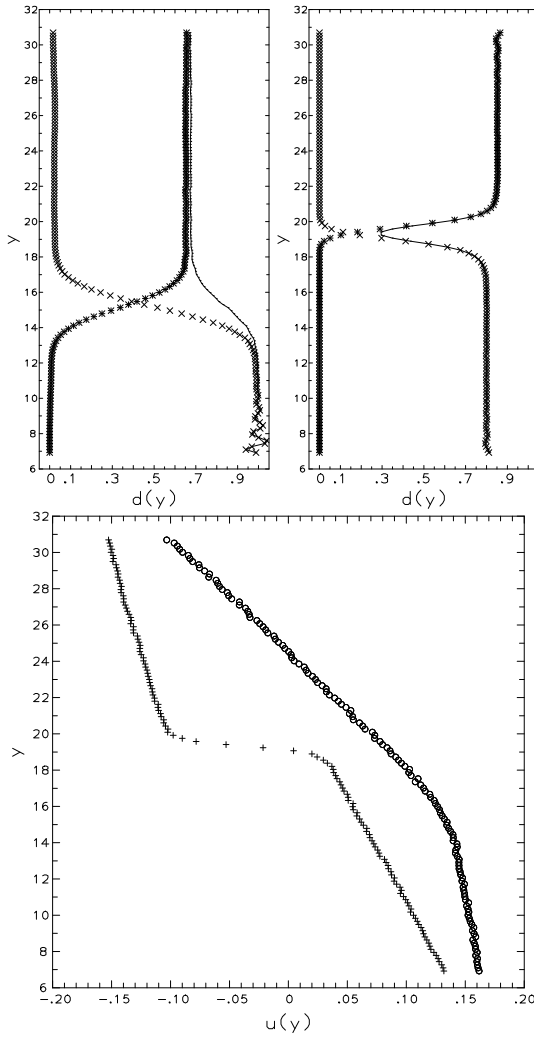


FIG. 2: Density and velocity profiles in Couette flow for (2,4) systems. The coordinate y runs normal to the interface, and the profiles average over the other two directions. In the density profiles, miscible (left) and immiscible (right), the (\times) symbols refer to the dimers and ($*$) to the tetramers, while the continuous curve is the total liquid density. In the velocity and other plots below, points labeled (o) and (+) refer to the miscible and immiscible systems, respectively.

tinuity, which we would describe precisely as ‘‘apparent velocity slip.’’ We have also simulated the same system at various wall velocities in the Couette case and twice the forcing in Poiseuille. The qualitative behavior of the snapshots and the density profiles are unchanged, while the magnitude of the velocity, apparent slip and stress scale roughly linearly, as indicated in Table I.

For the system with larger (4,16) molecules, the same qualitative picture applies – a monatomic density profile in the miscible case with no-slip velocity profiles, and a density dip accompanied by apparent slip in the immiscible case. The numerical values differ, and are recorded in

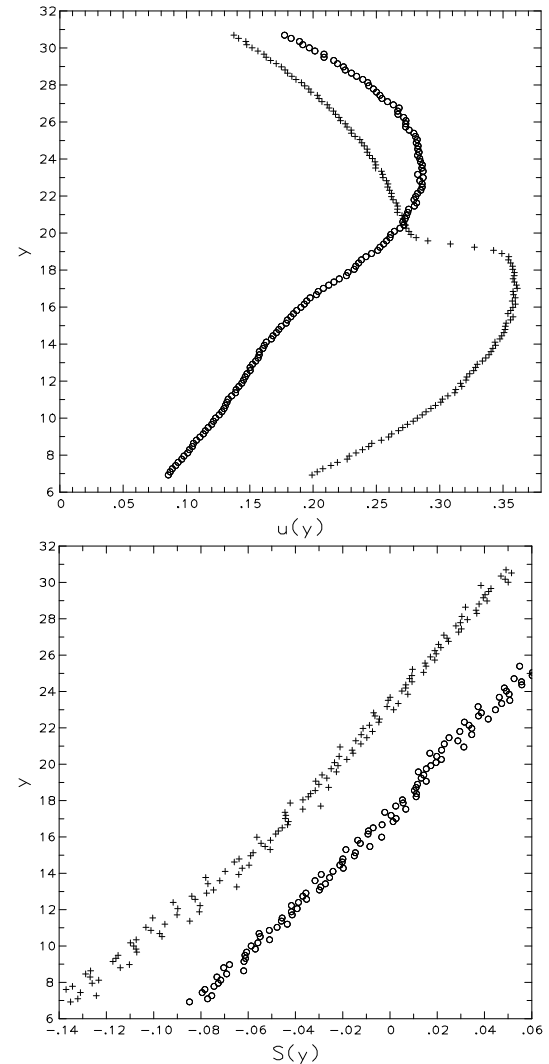


FIG. 3: Velocity and shear stress profiles in Poiseuille flow for the (2,4) systems, with points marked by (o) and (+) miscible and immiscible respectively.

Table I. The cases where slip occurs always have a dip in the total density at the liquid-liquid interface, but there is no monotonic relation between the numerical values in different systems. In the case of the purely monatomic (1,1) system, when the interactions are miscible the two liquids mix completely over the duration of the simulation [11]. For the immiscible interactions one sees a density dip similarly to that of the previous case, although of lesser magnitude (see Table I), and in Couette flow the velocity profile shows a rapid transition resembling that of Fig. 2. In Poiseuille flow however, the profile is a single parabola without any velocity slip. An explanation for this ostensibly inconsistent behavior is provided below.

It remains to characterize the velocity discontinuity in terms of a boundary condition suitable for continuum calculations. Following the history of the no-slip condition [1], simple plausibility, and the results of Zhao and

System	Flow	Δu	S	α	δ
(1,1)	0.001 C	0.0029	0.0011	2.6	0.49
	0.05 C	0.014	0.0059	2.4	0.49
	0.1 C	0.031	0.012	2.6	0.49
	0.2 C	0.050	0.020	2.5	0.49
	0.01 P	0.0	0.0	—	0.49
(2,4)	0.05 C	0.038	0.0063	6.0	0.66
	0.1 C	0.070	0.012	5.8	0.66
	0.2 C	0.13	0.021	6.2	0.66
	0.01 P	0.071	0.012	5.9	0.66
	0.02 P	0.15	0.025	6.0	0.66
(4,16)	0.1 C	0.032	0.0099	3.2	0.46
	0.2 C	0.070	0.021	3.3	0.46
	0.01 P	0.15	0.049	3.0	0.46
	0.02 P	0.22	0.70	3.1	0.46

TABLE I: Numerical results for slip. The notation is that (l_1, l_2) refers to a liquid made of flexible chains of length l_1 in contact with a second liquid of chains of length l_2 , with interactions either of the immiscible or miscible (LB) type. “0.1 C” means Couette flow with wall velocities ± 0.1 , and “0.01 P” means gravity driven Poiseuille flow with acceleration 0.01. Δu , S , α and δ are the apparent slip, shear stress at the interface, Navier coefficient and relative density dip, respectively. All entries are in MD units.

Macosko [6] for polymer systems, we consider the Navier condition $\Delta u = \alpha S$, where S is the shear stress at the position of the interface, and α is a slip coefficient that depends on the nature of the two liquids present. (α is the inverse of the coefficient β introduced in [6].) The more common form of the Navier condition at a solid-liquid interface follows from $S = \mu \partial u / \partial y$, where μ is the shear viscosity, and writing $\alpha = L\mu$ to define a slip-length L . In the liquid-liquid case, there are two viscosities in general, so this procedure is ambiguous, whereas the shear stress is unique and continuous across the interface. In the (1,1) immiscible system, the two liquids are identical except for their mutual repulsion and have equal viscosities and densities, so that the interface lies exactly in the middle of the channel. In Poiseuille flow, the shear stress then vanishes at the interface, and the Navier condition predicts no velocity discontinuity, exactly as seen in the simulations.

In Table I, we evaluate the slip coefficient from the MD data in the various cases simulated. The key feature of the Table is the approximately constant value of α obtained for each liquid pair, independent of the flow configuration and the value of the driving force. The numerical values have not been determined with very high precision, partly due to statistical fluctuations in the shear stress, and partly due to uncertainties in extrapolating across the interfacial region, but the trend is clear. At sufficiently high shear rates, non-Newtonian

effects would appear, and α might vary accordingly, as found in [6]. We conclude that the Navier condition is an appropriate and genuine boundary condition for a liquid-liquid interface.

An outstanding issue is the value of the slip coefficient α . If we use parameter values for Argon (for which the Lennard-Jones potential with $A_{ij} = 1$ is quantitatively valid) to translate the (1,1) coefficient into physical units, we have $\alpha \sim 10^{-5} \text{ m/Pa s}$, a value three orders of magnitude larger than observed or inferred in polymer melts [6, 7] at low shear rates. A likely explanation for the discrepancy is that the interactions used here may be too repulsive as compared to those in the experimental systems. To pursue this possibility, in the (2,4) system we ran additional simulations with decreasing immiscibility, using a sequence of higher values of the inter-liquid interaction strength $A_{12} = 0.2 \dots 0.8$. The apparent slip and the density dip were found to decrease roughly linearly to zero from their values at $A_{12} = 0$ in Table I. More generally, α depends in a non-trivial way on the molecular structure and interaction of both fluids present at the interface, as well as operating conditions such as temperature and density, and perhaps on driving force as well at higher shear and velocity, and little insight into its value is available at the moment.

We thank M. Rauscher for discussions and M. M. Denn for bringing Refs. [6, 7] to our attention. This work was supported by the NASA Exploration Systems Mission Directorate.

* Electronic address: koplik@sci.ccny.cuny.edu

† Electronic address: jayanth@phys.psu.edu

- [1] A recent survey is E. Lauga, M. P. Brenner and H. A. Stone, cond-mat/0501557, to appear in *Handbook of Experimental Fluid Dynamics*, ed. J. Foss, C. Tropea and A. Yarin (Springer, New York, 2005).
- [2] N. Giordano and J.-T. Cheng, *J. Phys.: Condens. Matter* **13**, R271 (2001).
- [3] H. A. Stone, A. D. Stroock and A. Adjari, *Annu. Rev. Fluid Mech.* **36**, 381 (2004).
- [4] E. H. Kennard, *Kinetic Theory of Gases* (McGraw-Hill, New York, 1938).
- [5] M. M. Denn, *Annu. Rev. Fluid Mech.* **33**, 265 (2001).
- [6] R. Zhao and C. W. Macosko, *J. Rheol.* **46**, 145 (2002).
- [7] Y. C. Lam, et al., *J. Rheol.* **47**, 795 (2003).
- [8] M. P. Allen and D. J. Tildesley, *Computer Simulation of Liquids* (Clarendon, Oxford, 1987).
- [9] J. Koplik and J. R. Banavar, *Annu. Rev. Fluid Mech.* **27**, 257 (1995).
- [10] M. Cieplak, J. Koplik and J. R. Banavar, *Phys. Rev. Lett.* **86**, 803 (2001).
- [11] The distinction between this case and the previous molecular (2,4) system is that the structure of the molecules make it difficult for the weakly interacting long chains to penetrate the densely packed region of short chains, although smaller spherical atoms can do so easily.